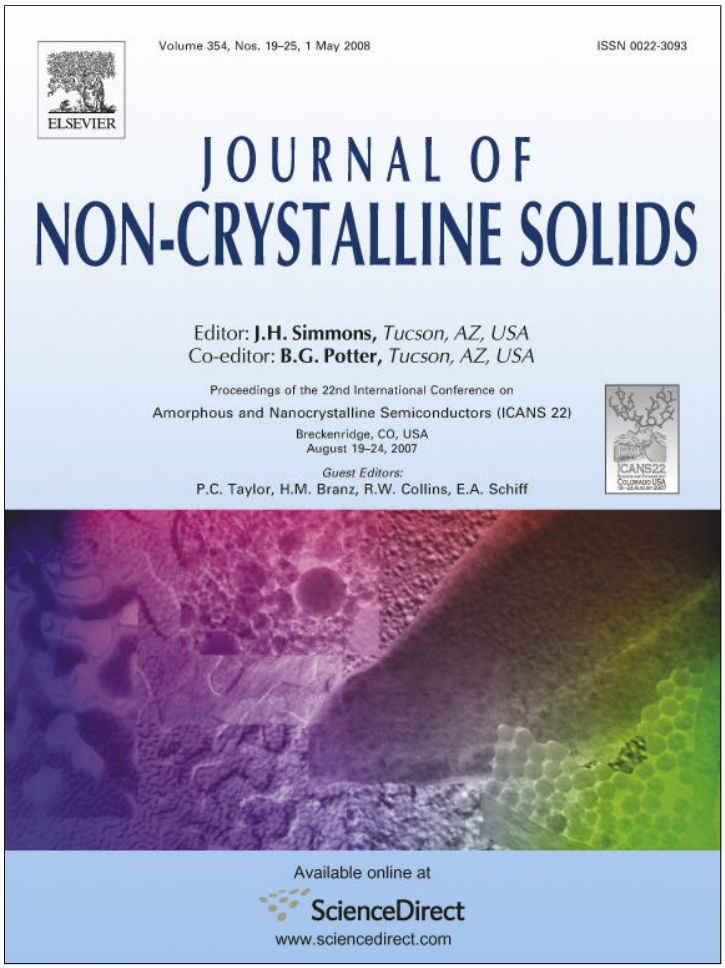

Available online at www.sciencedirect.com
ScienceDirect
Journal of Non-Crystalline Solids 354 (2008) 2691–2696
JOURNAL OF NON-CRYSTALLINE SOLIDS
www.elsevier.com/locate/jnoncrysol

Avalanche multiplication in amorphous selenium and its utilization in imaging

A. Reznik [a,*], S.D. Baranovskii [b], O. Rubel [b], K. Jandieri [b], S.O. Kasap [c], Y. Ohkawa [d], M. Kubota [d], K. Tanioka [d], J.A. Rowlands [e]

[a] Imaging Research, Sunnybrook Health Sciences Centre, 2075 Bayview Avenue, Toronto, Canada M4N 3M5
[b] Department of Physics and Material Sciences Center, Philipps University Marburg, D-35032 Marburg, Germany
[c] Department of Electrical Engineering, University of Saskatchewan, 57 Campus Drive, Saskatoon, SK, Canada S7N 5A9
[d] NHK Science and Technical Research Laboratories, 1-10-11 Kinuta, Satagaya-Ku, Tokyo 157-8510, Japan
[e] Toronto Sunnybrook Regional Cancer Centre, 2075 Bayview Avenue, Toronto, Canada M4N 3M5

Available online 31 January 2008

Abstract

Amorphous selenium (a-Se) is a well known photoconductor that is currently used in X-ray image detectors and HARP video tubes. Recent advances have made it practical to operate a-Se at extremely high electric fields F, where avalanche multiplication occurs. At sufficiently high fields, the effective quantum efficiency (η^*) (or the overall yield) of the photoconductor can be increased several orders of magnitude above unity and renders avalanche a-Se photoconductors a prospective alternative to vacuum photomultiplier tubes (PMTs) and silicon avalanche photodiodes (APDs). In this work we report our study of η^* and charge transport for a-Se avalanche photoconductors with different photoconductive layer thicknesses in wide range of F. Our study shows that a-Se is able to produce a gain of ~1000 with a rise time of ~1 ns, both of which clearly point to the potential (or realized) use of this photoconductor in a variety of imaging applications. Furthermore, our work supports the validity of the so-called modified Lucky drift model to explain the nature of impact ionization and avalanche in this material.

PACS: 71.55.Jv; 72.20.Jv; 72.20.Ht

Keywords: Amorphous semiconductors; Photoconductivity; Short-range order

1. Introduction

Avalanche multiplication in amorphous selenium (a-Se) was first discovered by Juska et al. more than 25 years ago on so-called a-Se insulating structures, where an a-Se photoconductive layer was sandwiched between two insulating polyethyleneteraphalate layers [1]. Insulating layers were necessary to avoid any possible charge injection from the contacts due to extremely high electric fields ($\geqslant 70$ V/μm) applied to a-Se layer to initiate and maintain the avalanche multiplication process. Although the experiments by Juska et al. unambiguously proved the existence of avalanche multiplication in a-Se, the insulating structures used at that time were not suitable for utilization of a-Se avalanche multiplication in practical imaging applications. Indeed, for practical use, the continuous photocurrent flow has to be provided, which is not possible with insulating layers. The first practical a-Se avalanche photosensor called a high-gain avalanche rushing photoconductor (HARP) utilizes a blocking structure [2], where a-Se layer is confined between two specially designed blocking contacts which prevent charge injection while providing the exit of photogenerated and multiplied carriers to the external electronic circuit.

* Corresponding author. Tel.: +1 416 480 6100x7129; fax: +1 416 480 5714.
E-mail address: alla.reznik@sunnybrook.ca (A. Reznik).

0022-3093/$ - see front matter © 2008 Elsevier B.V. All rights reserved.
doi:10.1016/j.jnoncrysol.2007.09.058

Fig. 1(a) shows the simplified diagram of a-Se photosensor which utilizes HARP layer. Photons in the visible range enter the a-Se layer from the transparent anode (indium tin oxide (ITO)) with most being absorbed within the first micron of the a-Se, creating electron-hole pairs (EHPs). Due to the direction of the applied electric field F, electrons are collected almost immediately by the anode and contribute little to the signal. Holes drift towards the negatively biased metal electrode on the other side of the layer, inducing an electrical current. For electric fields below the avalanche multiplication threshold ($F < \sim 70$ V/μm), the charge collected by the electrodes is equal to the number of EHPs created by the photons, resulting in a gain of unity. Above the avalanche multiplication threshold ($F > \sim 70$ V/μm), the drifting holes gain enough kinetic energy to create additional EHPs along their paths by impact ionization. This results in an exponential increase in the number of EHPs with traversed distance, that is, in avalanche multiplication, and consequently in internal gain. As it is seen from Fig. 1(a), a layer of a-Se is sandwiched between a thin layer of CeO_2 on the front side and Sb_2S_3 on the back. The CeO_2 blocks injection of holes from the positively biased ITO, and the Sb_2S_3 prevents electron injection. Due to the implementation of blocking contacts, the high electric field required for the initiation of avalanche multiplication is not accompanied by charge injection from bias electrodes: dark current is kept at a low value of <0.1 nA/mm^2.

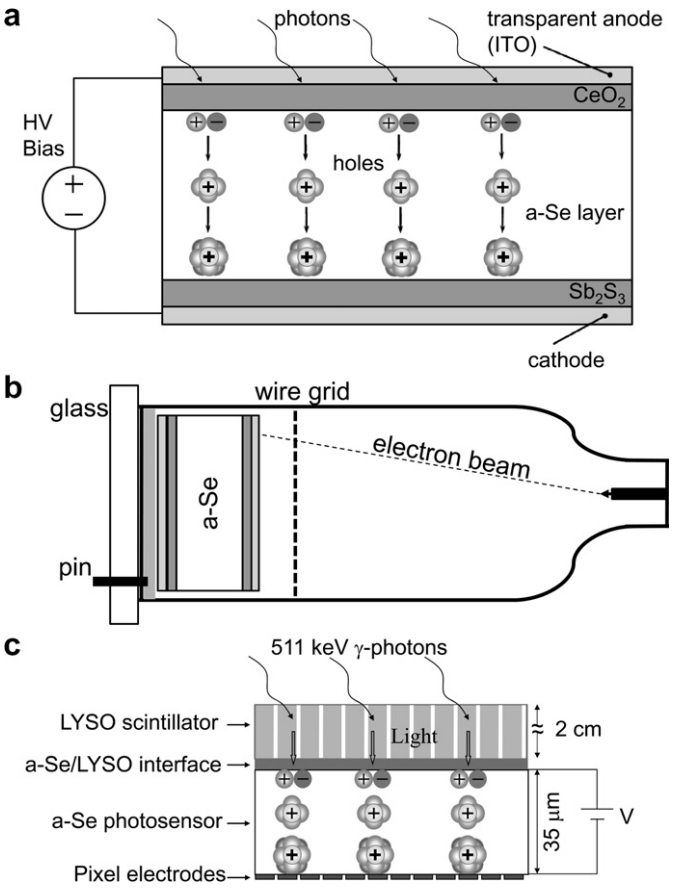

Fig. 1. Schematic diagram of avalanche a-Se photosensor (a), HARP TV tube (b) and a PET detector head with LYSO scintillation crystal and a-Se avalanche photosensor (not in scale) (c).

Currently a-Se HARP layers are employed in an electron-beam scanned Harpicon TV camera tubes. They were designed for news broadcasting when extremely low levels of light reach the image sensor. The schematic presentation of the Harpicon tube is shown in Fig. 1(b). The electric field across the a-Se layer is created by connecting a positive voltage supply to the connector pin of ITO layer acting as a transparent anode. There is no electrode on the back of the a-Se layer where photogenerated holes are accumulated forming a charge image. As the electron-beam scans the free surface and resets the accumulated charge, a current proportional to the amount of accumulated charge at the scan spot is detected. Thus, the harpicon readout is similar to that of a vidicon tube.

Avalanche a-Se blocking structures represent the future of a-Se photodetectors in medical X-ray and functional γ-ray imaging applications [3,4]. For these applications, avalanche a-Se photoconductors are intended to replace vacuum photomultipliers or silicon (Si) avalanche photodiodes (APDs) used to convert light emitted from a phosphor to charge. Fig. 1(b) shows the concept of use of a-Se avalanche photoconductor in indirect conversion sensors for positron emission tomography (PET). For this application, the a-Se avalanche photosensor is optically coupled to an array of advanced scintillator Cerium doped lutetium yttrium orthosilicate (LYSO). The principle of a-Se/LYSO detector operation can be described as follows:

When individual crystals of the LYSO array absorb incident γ-rays, a burst of optical photons is produced and guided by the geometry and surface treatment of the crystal, then impinge on the a-Se photoconductive layer (Fig. 1(c)). These photons are absorbed in a-Se very close to the a-Se/LYSO interface, and generate EHPs. The photogenerated holes are collected on a pixellated electrode array at the back a-Se surface where they form a latent charge image that is subsequently transferred to the readout electronic board (Fig. 1(c)).

To evaluate avalanche a-Se photosensors for their suitability as PET photodetectors, we performed a comprehensive study of the photoinduced response, including the avalanche gain and transient current. Photoconductive properties were studied for wavelengths of excitation $\lambda = 400$–450 nm to cover the emission range of advanced scintillation crystals used in advanced PET detectors.

In addition, the study of photoconductivity in a-Se in the avalanche regime is of fundamental scientific significance. Indeed, our understanding of the mechanism of impact ionization in this material is still incomplete although recently it has been possible to explain the fundamentals of impact ionization in amorphous solids in terms of the modified Lucky drift model. However, the complexity of impact ionization and avalanche formation in amor-

phous semiconductors continues to tax solid state theorists requiring new experimental results to clarify the effects.

2. Experimental results

2.1. Effective quantum efficiency of charge photogeneration

Effective quantum efficiency η^* of the photoconductor (also called the yield) was measured using a-Se phototargets from HARP tubes with thicknesses $d = 8$, 15, 25 and 35 μm. η^* encompasses both the primary mechanisms by which holes are released after photon absorption and the secondary mechanisms by which free holes can multiply. Fig. 2 shows the experimental setup. The front face of the a-Se was illuminated with photons of a specific energy (i.e. light of a specific wavelength, λ), produced using a grating monochromator. A constant light intensity (I) was maintained for each λ using a system of neutral density filters. These filters were adjusted automatically based on a feedback signal from a calibrated photodiode prior to each measurement. We used a HARP substrate with no a-Se deposited on it, in a separate control experiment to measure the transmission (T) through the layers in front of the a-Se, as a function of λ. The parameter T was taken into account in the calculation of η^*.

Electrons and holes in the a-Se were separated by an adjustable electric field, applied by connecting a positive voltage supply to the ITO electrode at the front surface. Mobile holes travel through the a-Se, and in a HARP camera produce a positive surface charge on the free surface at the rear. A photocurrent (I_{ph}) was measured through a capacitively coupled tap at the ITO electrode, while a scanning electron-beam controlled by the camera's electronics made contact at the free surface, thereby closing the circuit.

Effective quantum efficiency was calculated from I_{ph} using the following expression:

$$\eta^* = \frac{I_{ph}/e}{IT/hv}, \tag{1}$$

where e is the elementary charge, hv is the incident photon energy.

Fig. 3 shows η^* for $\lambda = 420$ nm (which corresponds to the peak emission from LYSO crystal) plotted as a function of electric field for four selected a-Se layer thicknesses. At comparatively low electric fields η^* increases with increasing F and at $F \sim 40$ V/μm η^* saturates at unity. For the limited F range before hole avalanche multiplication begins, η^* is field independent. The onset of avalanche multiplication F_{av} manifests itself by a sharp increase in η^* above unity. F_{av} is thickness dependent: while for comparatively thin films avalanche multiplication begins at ~80 V/μm, for thicker films ($d > 30$ μm) holes start to avalanche at slightly lower fields (~70 V/μm).

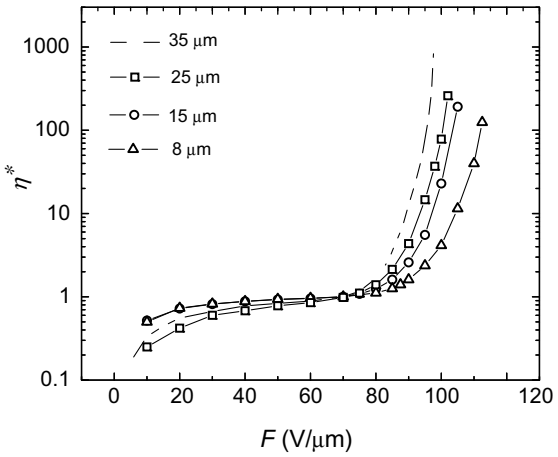

Fig. 3. Field dependence of effective quantum efficiency of photogeneration at 420 nm of excitation for different a-Se layer thicknesses.

Since $\eta^* \sim 1$ even in the sub-avalanche regime (i.e. at $F < 70$ V/μm), the avalanche gain g_{av} can be calculated by the following relationship:

$$g_{av}(F) = \eta^*(F)/\eta^*\ (70\ \text{V}/\mu\text{m}), \tag{2}$$

where $\eta^*(70\ \text{V}/\mu\text{m})$ is η^* at $F = 70$ V/μm. Fig. 4 shows g_{av} for different a-Se layer thicknesses ($d = 8$, 15, 25 and 35 μm) for a given electric field of 90 V/μm. The linear dependence of $\log(g_{av})$ as function of d proves that g_{av} follows an exponential dependence on the a-Se thickness, indicating that just one type of carrier, namely, holes, undergo avalanche multiplication:

$$g_{av} = \exp(\gamma_p d), \tag{3}$$

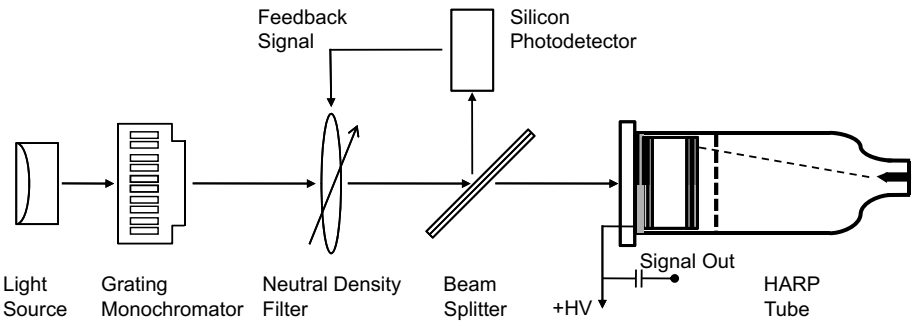

Fig. 2. Experimental apparatus for measurement of electron-hole pair production in a-Se. Single-wavelength light is incident on the a-Se target of the HARP tube. Photoconductor current is recorded as a function of the high voltage (HV) applied across the a-Se. When measurements are performed for different wavelengths of light, the incident light intensity is kept constant by monitoring a feedback signal.

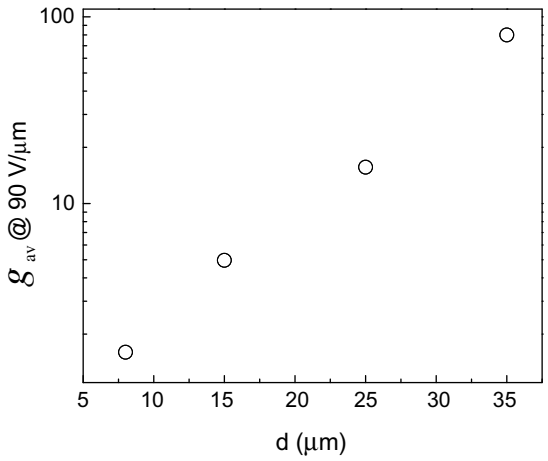

Fig. 4. Thickness dependence of avalanche multiplication gain measured at 90 V/μm.

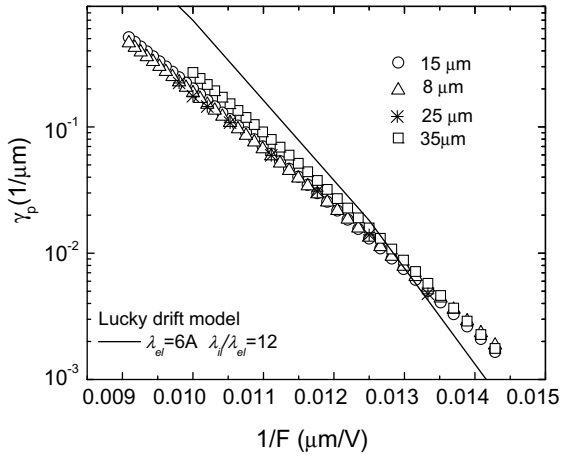

Fig. 5. Field dependence of hole impact ionization coefficient for different a-Se layer thicknesses.

where γ_p is a field depended impact ionization coefficient (IIC) for holes.

Thus, we can calculate the field dependence of γ_p using the experimentally determined η^* vs. F dependence. The results are shown in Fig. 5 (symbols). Both strong dependence of γ_p on F and its independence on d are evident from Fig. 5.

2.2. Charge transport

A conventional time-of-flight (TOF) experiment was performed to measure the hole mobility in a-Se. In this experiment, the transient current produced by the a-Se phototarget of a HARP tube in response to an impulse excitation (337.1 nm, 800 ps, 1.65 mJ) was measured. Due to the high absorption coefficient of a-Se at 337 nm, carriers are generated at the surface of the sample, so holes traverse a distance equal to d. To prevent the accumulation of holes, the back of the target is discharged by a scanning electron-beam. The duration of the laser pulse was shorter than the transit time for holes under all our experimental conditions. All TOF traces were recorded on a 2.5 GHz bandwidth digital oscilloscope.

TOF measurements were performed at temperatures between 25 °C and 40 °C. Conditions above room temperature were produced via external heating of the a-Se target with a hot air gun. The limit of stable camera operation dictated the upper limit of the temperature range.

Fig. 6 shows an example of the measured charge collection curves, which were obtained by integrating the transient current in the sub-avalanche regime: (a) ($F = 15$ V/μm) and avalanche regime (b) ($F = 100$ V/μm). Well pronounced knee in Fig. 6(a) defines hole transit time in non-avalanche regime. The shape of charge collected curve in avalanche regime is different from that in non-avalanche regime. The fast leading edge due to the collection of ava-

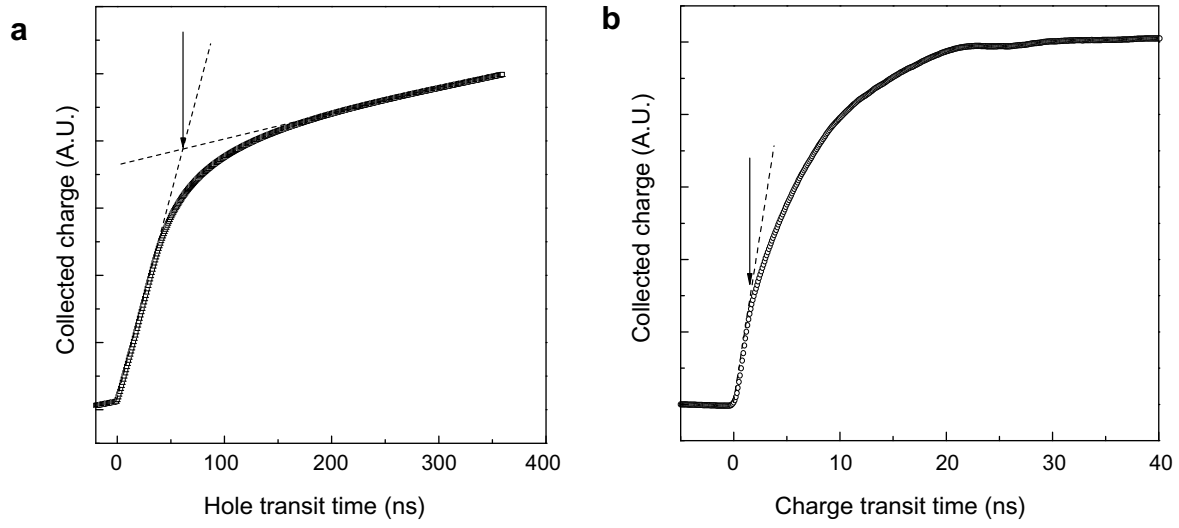

Fig. 6. Charge collection curves in the sub-avalanche regime ($F = 15$ V/μm) (a) and avalanche regime ($F = 100$ V/μm) (b). Arrows indicate hole transit time.

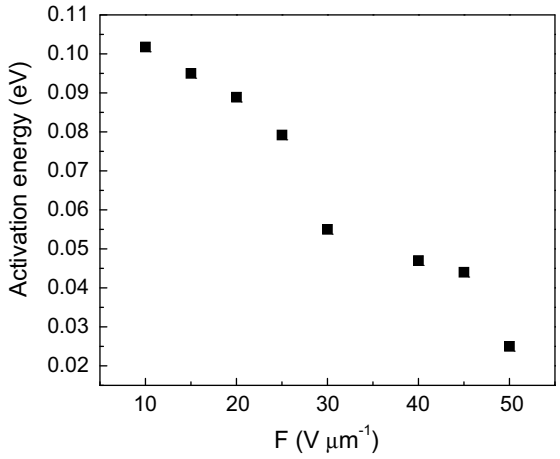

Fig. 7. Field dependence of the activation energy of hole mobility in a-Se HARP layers.

lanching holes is followed by less rapidly growing part due to the slow collection of secondary electrons which are created in the trail of avalanching holes.

Measurements of hole transit times allows to derive drift hole mobility

$$\mu = \frac{d}{t_h F}, \tag{4}$$

which shows slight thermal activation behaviour. The activation energy of hole mobility ε_a over the limited temperature range was found to be field dependent (Fig. 7): ε_a decreases with increase in F resulting in hole transport deactivation at ~50 V/μm.

3. Discussion

There are two competing models that can to account for avalanche multiplication in amorphous media, namely, the modified Lucky drift (LD) model [5] and the polaron model suggested recently for switching effect in a non-uniform media [6]. The main peculiarity of the modified LD model is that, in contrast to the conventional LD model, it differentiates between elastic scattering on disorder potential and inelastic scattering on optical phonons. This allows a drifting carrier to lose just a portion of its kinetic energy on inelastic collisions with phonons thus permitting to gain enough energy to initiate impact ionization while travelling along the field. In contrast, the polaron model suggests that switching to a high-conducting state in a non-uniform media can be due to the increase in the concentration of small polarons converting the latter into free carriers.

We believe that our experimental results allow us to rule out polaron mechanism as a possible mechanism for avalanche multiplication in a-Se. Indeed, in accordance with the polaron model, transport deactivation has to be concurrent with the transition into a high-conducting state. However, this is obviously not the case of a-Se, where hole transport becomes deactivated well before avalanche multiplication begins: as it is seen from Fig. 7 hole mobility deactivation occurs at ~50 V/μm, while avalanche multiplication starts at much higher electric fields (at least at 70 V/μm for thick a-Se layers). Since polaron transport is thermally activated, one has to conclude that there is no polaron contribution to charge transport in a-Se at electric fields above ~50 V/μm. In contrast, hole transport deactivation prior to the onset of impact ionization agrees well with the modified Lucky drift model. In accordance with modified LD model, hole transport deactivation at comparatively low electric fields is required as a precursor for the beginning of avalanche multiplication. Indeed, there has to be an intermediate 'heating' regime when holes are not trapped anymore into the localised states within the band tails, but move with a microscopic mobility. The latter occurs in the field region between 50 and 70 V/μm.

The further proof of the validity of the modified LD model for impact ionization in a-Se is provided by the photocurrent behaviour in the avalanche regime. As can be seen from Fig. 6(b) fast avalanching holes and slow non-avalanching electrons do contribute to the photocurrent in this regime. This agrees well with the modified LD model which suggests that impact ionization occurs across the mobility gap. The latter necessarily results in the creation of free mobile holes as well as free mobile electrons. Fitting of our experimentally measured IIC for holes γ_p (see solid line in Fig. 5) permits for an estimation of the mean free paths for the elastic (λ_{el}) and inelastic (λ_{ie}) scattering processes which appear to be 6 Å and 72 Å, respectively. Although λ_{el} are λ_{ie} are treated as free parameters in the modified LD model their values are reasonable and do not contradict with amorphous semiconductor basic physics. Indeed, λ_{el} has to be on the interatomic scale while λ_{ie} has to correspond to a phonon frequency $v \sim 10^{12}$ s^{-1}:

$$\lambda_{ie} = \mu \times F \times v^{-1}. \tag{5}$$

The estimate of λ_{ie} for $\mu \cong 1$ cm^2/V s [7] and $F = 100$ V/μm gives the value of 100 Å, which is in remarkable agreement with the estimations provided by the modified LD model.

4. Conclusions

Experimental results on charge transport and impact ionization in a-Se are reported. The consistency with the modified Lucky Drift model is shown.

Acknowledgements

Authors are grateful to Dr G. Juska for fruitful discussions. A.R. gratefully acknowledges the financial support of the Susan G. Komen Brest Cancer Foundation (Grant # BCTR0504418) and Cancer Care Ontario (CINO). Financial support of the Fonds der Chemischen Industrie and that of the Deutsche Forschungsgemeinschaft is gratefully acknowledged.

References

[1] G. Juska, K. Arlauskas, Phys. Stat. Sol. (a) 59 (1980) 389.
[2] M. Kubota, T. Kato, S. Suzuki, H. Maruyama, K. Shidara, K. Tanioka, K. Sameshima, T. Makishima, K. Tsuji, T. Hirai, T. Yoshida, IEEE Trans. Broadcast. 42 (3) (1996) 251.
[3] W. Zhao, D. Li, A. Reznik, B.J.M. Lui, D.C. Hunt, Y. Ohkawa, K. Tanioka, J.A. Rowlands, Med. Phys. 32 (9) (2005) 2954.
[4] A. Reznik, B.J.M. Lui, J.A. Rowlands, Technol. Cancer Res. Treat. 4 (2005) 61.
[5] O. Rubel, S.D. Baranovskii, I.P. Zvyagin, P. Thomas, S.O. Kasap, Phys. Stat. Sol. (c) 5 (2004) 1186.
[6] D. Emin, Phys. Rev. B 74 (2006) 035206.
[7] A. Cesnys, G. Juska, E. Montrimas, in: R. Fairman, B. Ushkov (Eds.), Semiconducting Chalcogenide Glass II : Properties of Chalcogenide Glasses, Elsevier, Academic, 2004, p. 15.